SPANDIDOS PUBLICATIONS

MOLECULAR MEDICINE REPORTS 30: 201, 2024

ARID1A overexpression inhibits colorectal cancer cell migration through the regulation of epithelial-mesenchymal transition

SASITHORN WANNA-UDOM[1], SIRIPAT ALUKSANASUWAN[2,3], KEERAKARN SOMSUAN[2,3], WARIYA MONGKOLWAT[1] and NATTHIYA SAKULSAK[1,4]

[1]Department of Anatomy, Faculty of Medical Science, Naresuan University, Phitsanulok 65000, Thailand; [2]School of Medicine, Mae Fah Luang University, Chiang Rai 57100, Thailand; [3]Cancer and Immunology Research Unit, Mae Fah Luang University, Chiang Rai 57100, Thailand; [4]Faculty of Medicine, Praboromarajchanok Institute, Ministry of Public Health, Nonthaburi 11000, Thailand

Received May 3, 2024; Accepted August 9, 2024

DOI: 10.3892/mmr.2024.13325

Abstract. The advancement of tumor cell metastasis is significantly influenced by epithelial-to-mesenchymal transition (EMT), and metastasis is a prominent contributor to the mortality of patients diagnosed with colorectal cancer (CRC). AT-rich interactive domain-containing protein 1A (ARID1A), which acts as a tumor suppressor, frequently exhibits a loss-of-function mutation in metastatic CRC tissues. However, the underlying molecular mechanisms of ARID1A relating to EMT remain poorly understood. The present study aimed to clarify the association between ARID1A and EMT regulation in human CRC cells. The investigation into the loss of ARID1A expression in tissues from patients with CRC was performed using immunohistochemistry. Furthermore, *ARID1A*-overexpressing SW48 cells were established using lentiviruses carrying human full-length *ARID1A*. The results revealed that overexpression of *ARID1A* induced cellular morphological changes by promoting the tight junction molecule zonula occludens 1 (ZO-1) and the adherens junction molecule E-cadherin, whereas it decreased the intermediate filament protein vimentin. The results of reverse transcription-quantitative PCR also confirmed that *ARID1A* overexpression upregulated the mRNA expression levels of *TJP1*/ZO-1 and *CDH1*/E-cadherin, and downregulated *VIM*/vimentin and zinc finger E-box binding homeobox 1 expression, which are considered epithelial and mesenchymal markers, respectively. In addition, the overexpression of *ARID1A* in CRC cells resulted in a suppression of cell motility and migratory capabilities. The present study also demonstrated that the tumor suppressor ARID1A was commonly absent in CRC tissues. Notably, *ARID1A* overexpression could reverse the EMT-like phenotype and inhibit cell migration through alterations in EMT-related markers, leading to the inhibition of malignant progression. In conclusion, ARID1A may serve as a biomarker and therapeutic target in the clinical management of metastatic CRC.

Correspondence to: Dr Natthiya Sakulsak, Faculty of Medicine, Praboromarajchanok Institute, Ministry of Public Health, 47/99 Building 7, Tiwanon Road, Talad Kwan, Mueang, Nonthaburi 11000, Thailand
E-mail: natthiyak@nu.ac.th, natthiyas@pi.ac.th

Key words: colorectal cancer, AT-rich interactive domain-containing protein 1A, epithelial-mesenchymal transition, epithelial-mesenchymal transition-related markers, cell migration

Introduction

Colorectal cancer (CRC) is a common cause of cancer morbidity and mortality; it is the third most frequently diagnosed malignancy worldwide and the second most common cause of cancer-related mortality (1-3). According to global cancer statistics, >1.85 million new cases of CRC (9.8% of total cancer cases) and an estimated 850,000 CRC-related deaths (9.2% of total cancer-related deaths) occurred in 2020 (2,4). Among patients with CRC, 20% have metastatic CRC and 40% present with recurrence after previous localized disease treatment. Notably, prognosis of metastatic CRC is poor, with a 5-year survival rate of <20% (5), and these patients often develop resistance to systemic therapy. Moreover, 35-40% of patients with *KRAS* and *NRAS* gene mutations do not respond to targeted therapy (5,6). CRC is a heterogeneous disorder characterized by a variety of molecular alterations, including the dysregulation of signaling pathways, leading to tumor initiation, development and metastasis (7). Therefore, it is important to identify and develop measures to effectively prevent the metastasis of CRC cells. Understanding the pathogenesis of CRC and the expression of related molecules is also required to develop molecular therapies for the treatment of metastatic CRC.

The AT-rich interactive domain-containing protein 1A (*ARID1A*) gene encodes the BAF250a protein, one of the accessory subunits of the SWItch/Sucrose Non-Fermentable chromatin-remodeling multi-subunit complex (8), which specifically modulates promoter accessibility for transcriptional gene activation or suppression, and regulates multiple cellular processes, including development, proliferation, differentiation, DNA repair and tumor suppression (9,10). Mutations in these subunits can result in abnormal control of lineage-specific differentiation and gene expression/suppression, contributing

to tumorigenesis in different types of cancer (8). According to next-generation sequencing, *ARID1A* has been identified as a frequently mutated gene in various types of cancer, including ovarian clear cell carcinoma (11), breast cancer (12), hepatocellular carcinoma (13), esophageal adenocarcinoma (14) and CRC (15). Furthermore, it has become increasingly clear that ARID1A variation is associated with the clinicopathological features of CRC (16,17). In patients with CRC, the loss of ARID1A expression has been reported to be more significant as the tumor-node-metastasis (TNM) stage advances (16), indicating that loss of ARID1A in CRC could be strongly associated with tumor progression and metastasis. However, the precise molecular mechanisms through which ARID1A contributes to the metastasis of CRC remain poorly elucidated.

Epithelial-mesenchymal transition (EMT) is a highly dynamic and reversible mechanism that favors malignant cancer behaviors, such as invasion and metastasis (18). It is a biological process in which epithelial cells exhibit downregulation of their epithelial properties and an increase in mesenchymal properties, which is mainly triggered by cytokines and growth factors secreted by the tumor microenvironment (19,20). In CRC, EMT is associated with tumor invasion, metastasis and resistance to chemotherapy (21). Previous studies have established a significant association between ARID1A and EMT. Notably, it has been revealed that the suppression of ARID1A can enhance migratory capabilities by facilitating EMT in both breast and gastric cancer cells (22,23); however, its mechanisms of action in CRC remain to be elucidated. Hence, the role of ARID1A in the regulation of EMT deserves consideration. Additionally, the potential involvement of ARID1A in CRC through its impact on the EMT mechanism has garnered attention. Therefore, the present study conducted experiments to examine the function of ARID1A in CRC and to offer preliminary guidance for targeted therapies in the clinical management of metastatic CRC.

Materials and methods

Patient samples. A total of 20 samples of formalin-fixed, paraffin-embedded (FFPE) CRC tissue blocks were provided by Dr Ratirat Samol (Unit of Pathology, Sawanpracharak Hospital, Nakhon Sawan, Thailand). The preparation of FFPE blocks was conducted by the hospital's pathological laboratory following standard procedures. These samples were diagnosed with different pathological grades of CRC between January and December 2021, with samples obtained from 9 men and 11 women (age range, 61-97 years). The research procedures involving individuals were granted approval by the Human Ethics Review Board of Sawanpracharak Hospital (approval no. 16/2560) and the Naresuan University Ethical Committee for Human Research (Phitsanulok, Thailand; approval no. P1-0191/2564; certificate of approval no. 178/2021), and adhered to the principles outlined in The Declaration of Helsinki.

Immunohistochemistry (IHC) and scoring. IHC was performed on 3-μm FFPE tissue sections from patients with CRC using a rabbit anti-human ARID1A antibody (1:400 dilution; cat. no. HPA005456; MilliporeSigma). Briefly, the sections underwent deparaffinization with xylene followed by rehydration in a decreasing concentration of alcohol solutions. The sections underwent heat-induced epitope retrieval with citrate buffer (pH 6) for 15 min at 97˚C. Subsequently, endogenous enzyme activity was quenched with 3% H_2O_2/NaN_3 for 25 min and non-specific reactivity was blocked with 0.1% NaN_3 for 20 min at room temperature, followed by the primary antibody incubation at 4˚C overnight in a humidified chamber. The bound antibody was then detected using a goat anti-rabbit IgG (H+L) antibody [Rabbit specific HRP/DAB Detection IHC Kit; cat. no. ab64261; Abcam] for 15 min at room temperature. A positive reaction was developed with ready-to-use DAB substrate (cat. no. ab64238; Abcam) for 3 min at room temperature. The sections were subsequently counterstained with hematoxylin, by briefly dipping the sections in this solution twice. The staining results were observed under a light microscope, with five distinct areas in both the cancerous and non-cancerous regions of CRC tissues systematically captured (Carl Zeiss AG; magnification, x400).

The immunostained sections were evaluated and assessed by an expert pathologist, who was blinded to the clinicopathological information of the patients, according to the percentage of stained cells and the intensity of staining. The IHC staining intensity was based on the histochemical scoring (H-score) assessment and was conducted utilizing a four-point grading system that assesses the staining intensity of the cells, as follows: Negative staining (0), weak positive staining (1), moderate positive staining (2), and strong positive staining (3). The H-score was calculated using the following formula: H-score=[(0x % negative cells) + (1x % weak positive cells) + (2x % moderate positive cells) + (3x % strong positive cells)]. The H-score representing IHC staining intensity was compared between cancerous and adjacent non-cancerous areas on the same tissue slide.

Cell culture, plasmids, transfection and transduction. SW48 CRC cells and 293 expressing the large T-antigen of simian virus 40 (293T) cells were obtained from the American Type Culture Collection. The cells were maintained in Dulbecco's modified Eagle's medium supplemented with 10% fetal bovine serum (FBS), 100 μg/ml streptomycin and 100 U/ml penicillin (all from Gibco; Thermo Fisher Scientific, Inc.) at 37˚C in a humidified chamber containing 5% CO_2.

The lentivirus-mediated gene overexpression (pLenti-puro-ARID1A; cat. no. 39478) and empty vector (pLenti-puro; cat. no. 39481) systems were purchased from Addgene, Inc., with lentiviral vectors carrying puromycin tags. For the 2nd-generation lentiviral system, the lentiviral vectors were co-transfected into 293T cells with pCMV-VSV-G and psPAX2 plasmids (Addgene, Inc.) in a 1.5:1:1 μg ratio, using Lipofectamine® 3000 (Invitrogen; Thermo Fisher Scientific, Inc.). After 16 h at 37˚C, the cell culture media was refreshed. A total of 48 h after transfection, the harvested viral supernatants were centrifuged at 2,000 x g for 5 min at 4˚C, filtered through 0.45-μm membrane filters, and transduced into SW48 cells at a multiplicity of infection of 2.5, utilizing 8 mg/ml polybrene reagent (MilliporeSigma). A total of 24 h post-transduction, the lentivirus-infected cells were selected in selection medium containing 500 ng/ml puromycin (Invitrogen; Thermo Fisher Scientific, Inc.) for 3-5 days. The remaining living cells were collected and used in the subsequent experiments.

Table I. Sequences of primers used in reverse transcription-quantitative PCR analysis of gene expression.

Gene	NCBI accession no.	Forward, 5'-3'	Reverse, 5'-3'	Product size, bp
ARID1A	NM_006015.6	TCCCACCTGGCTCTGTTGAA	CATCATTACCCGCCATGCC	101
CDH1	NM_004360.5	ATTTTTCCCTCGACACCCGAT	TCCCAGGCGTAGACCAAGA	109
TJP1	NM_003257.5	CCCTCAAGGAGCCATTC	CAGTTTGCTCCAACGAGA	264
VIM	NM_003380.5	CCTTGAACGCAAAGTGGAATC	AGGTCGGGCTTGGAAACATC	138
ZEB1	NM_001128128.3	ACCCTTGAAAGTGATCCAGC	TTGGGCGGTGTAGAATCAGA	111
GAPDH	NM_002046.7	CGACCACTTTGTCAAGCTCA	AGGGGTCTACATGGCAACTG	228

ARID1A, AT-rich interactive domain-containing protein 1A; *VIM*, vimentin; *ZEB1*, zinc finger E-box binding homeobox 1.

Cell staining and immunofluorescence. Lentivirus-infected SW48 cells were fixed in 4% paraformaldehyde for 10 min and stained with 0.4% crystal violet for 30 min at room temperature, facilitating the observation of morphological changes through a light microscope (Olympus IX70; Olympus Corporation). The expression of EMT protein markers was observed in *ARID1A*-overexpressing SW48 cells by immunofluorescence staining. Cells were grown in a 96-well plate until they reached 50% confluence within 48 h, after which, they were rinsed with 1X PBS and then fixed with 4% paraformaldehyde for 30 min at room temperature. After fixation, the cells underwent two washes with 1X PBS. Subsequently, they were permeabilized with 0.2% Triton X-100 solution for 5 min and nonspecific immunoreactivity was blocked with 2% bovine serum albumin (MilliporeSigma) for 1 h at room temperature. The cells were then exposed individually to primary antibodies against E-cadherin (1:1,000 dilution; cat. no. ab40772; Abcam), zonula occludens 1 (ZO-1; 1:1,000 dilution; cat. no. ab216880; Abcam), vimentin (1:500 dilution; cat. no. ab92547; Abcam) and zinc finger E-box binding homeobox 1 (ZEB1; 1:500 dilution; cat. no. ab203829; Abcam) overnight at 4˚C. After washing with PBS three times, the bound antibodies were visualized using Alexa Fluor® 488-conjugated goat anti-rabbit IgG antibody (1:1,000 dilution; cat. no. A11008; Invitrogen; Thermo Fisher Scientific, Inc.) for 1 h at room temperature in the absence of light. Subsequent counterstaining was performed with 1 μg/ml DAPI for 30 min in the dark. Finally, the fluorescent images were visualized using a laser scanning confocal microscope (Carl Zeiss™ AXio Vert.A1; Carl Zeiss AG).

Reverse transcription-quantitative PCR (RT-qPCR). Total RNA was extracted from sub-confluent cell cultures with TRIzol® reagent (Invitrogen; Thermo Fisher Scientific, Inc.) according to the manufacturer's guidelines. The isolated RNA was quantified using a NanoDrop ND-1000 spectrophotometer (NanoDrop Technologies) and cDNA was then synthesized using a SuperScript Vilo cDNA synthesis kit (Invitrogen; Thermo Fisher Scientific, Inc.), according to the manufacturer's protocol. The Luna Universal qPCR Master Mix (New England BioLabs, Inc.) was utilized to perform qPCR using the CFX96™ Optics Module (Bio-Rad Laboratories, Inc.). Gene amplification was carried out according to the standard instructions: An initial DNA denaturation step at 95˚C for 3 min; 40 cycles of denaturation at 95˚C for 15 sec, annealing at 60˚C for 30 sec and extension at 72˚C for 30 sec; followed by a melt curve (58-95˚C). All RT-qPCR assays were performed in duplicate and were repeated in at least three independent experiments. The relative fold gene expression levels of the samples were calculated using the $2^{-\Delta\Delta Cq}$ method (24) and were normalized to the control, human *GAPDH* expression. The specific oligonucleotide primer sequences are presented in Table I.

Wound healing assay. Cells were placed in a 24-well plate and incubated for 24 h at a final cell density of 80%. The cell surface was gently scratched across the center of the well with a 200-μl sterile pipette tip to create an equally wide single scratch. The plate then underwent three washes with PBS in order to eliminate any detached cells and debris. To facilitate the survival of the cells, they were subsequently cultured with fresh culture medium supplemented with 10% FBS (25) and were incubated in a humidified incubator containing 5% CO_2 at 37˚C. Areas of wound healing were examined under an inverted light microscope (Olympus IX70; Olympus Corporation) and images were captured immediately after the scratch was generated (T0), as well as at 24 h (T24), 48 h (T48) and 72 h (T72) after incubation at 37˚C using imaging software (magnification, x100; cellScens Standard.Ink, version 2.3; Olympus Corporation). The images of the same areas were acquired. The change in cell-free area and wound closure rate were calculated by referring to the image at T0 using ImageJ (version no. 1.54 g; National Institutes of Health) (26).

Transwell cell migration assay. Cell migration was measured in SPLInsert™ Hanging 8.0-μm pore polycarbonate membrane inserts (SPL Life Sciences). Vector control or *ARID1A*-overexpressing cells were seeded into the insert at a density of $2x10^4$ cells/well in serum-free medium (upper chamber). The insert was then transferred into a 24-well plate containing culture medium supplemented with 10% FBS (lower chamber). After incubation in a humidified atmosphere at 37˚C for 24 h, cells remaining on the surface of the upper chamber that had not penetrated the filter were removed with a cotton swab. The cells that had migrated to the lower surface of the insert were fixed with 4% paraformaldehyde for 2 min at room temperature, followed by a 20-min permeabilization with 100% methanol at room temperature. Subsequently, the samples were washed with PBS and stained with 0.4% crystal violet dye for 15 min at room temperature. The migrated cells

were observed and images were captured under a bright-field microscope. The number of migrating cells in each chamber was quantified by counting from at least four fields and three experiments, using ImageJ software analysis (26).

Statistical analysis. Three independent experiments were performed. Results are presented as the mean ± standard deviation or mean ± standard error of the mean. Statistical analysis was conducted using GraphPad Prism version 9.5.1 (Dotmatics). To test for differences in ARID1A protein expression, a paired t-test was used to compare variance in cancerous and adjacent non-cancerous areas from the same CRC tissues. Differences between two independent groups were analyzed using Student's t-test, whereas multiple comparisons between >2 groups were assessed using one-way analysis of variance and Tukey's post hoc test. P<0.05 was considered to indicate a statistically significant difference.

Results

ARID1A exhibits a low expression in human CRC tissues. Since mutations in *ARID1A* have been demonstrated to result in the absence of protein expression in tumors (11-15), the expression of ARID1A in CRC tissues was initially investigated. IHC was employed to analyze the expression levels of ARID1A in the cancerous regions (n=20), as well as in the corresponding adjacent non-cancerous regions (n=20) of tissues. All CRC tissues exhibited ARID1A expression in adjacent normal mucosal epithelial cells, with strong, moderate and weak positive staining observed in 11 cases (55%), 8 cases (40%) and 1 case (5%), respectively. By contrast, ARID1A expression was detected in cancerous regions, with strong, moderate and weak positive staining observed in 1 case (5%), 14 cases (70%) and 5 cases (25%), respectively. These data revealed that ARID1A exhibited a lower expression in the cancerous regions (Fig. 1B) than in the adjacent normal areas (Fig. 1A). Similarly, the average H-score of ARID1A, as determined by IHC, was significantly lower in cancerous areas than that in the adjacent non-cancerous regions (P<0.0001; Fig. 1C). ARID1A expression was reduced in CRC tissues, probably due to the fact that *ARID1A* is frequently mutated in CRC (15). Moreover, the loss of ARID1A has been shown to be closely linked to CRC metastasis (16). The subsequent experiments focused on the process of EMT and its association with CRC metastasis, specifically focusing on the involvement of ARID1A.

Overexpression of ARID1A is associated with morphological alterations in SW48 cells. To distinguish the effect of ARID1A on an EMT-like phenotype in CRC, SW48 cells were transduced with a lentivirus expressing human full-length *ARID1A*, and its overexpression was confirmed by RT-qPCR. The mRNA expression levels of *ARID1A* were increased by ~2-fold in SW48 cells that overexpressed *ARID1A*, confirming the successful establishment of *ARID1A*-stabilized cells (Fig. 2A). Cell morphology was observed under a phase-contrast microscope following 0.4% crystal violet staining. Control lentivirus-infected SW48 cells originally exhibited an epithelial phenotype with concentric nuclei and the cytoplasm was spread out in a uniform direction; in addition, the shape of the cells was round, cuboid or columnar (Fig. 2B). However, SW48

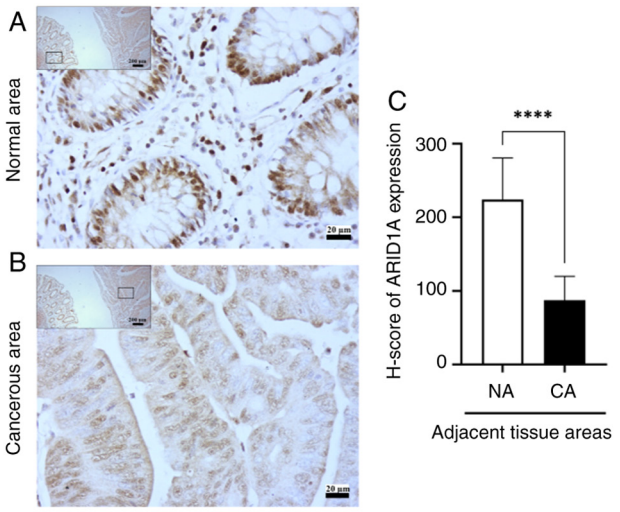

Figure 1. ARID1A expression is lost in CRC tissues. (A) ARID1A expression in normal tissue areas adjacent to cancerous tissue areas. (B) Low expression of ARID1A in the cancerous region of tissues. Original magnification, x400; scale bar, 20 μm. (C) H-score of IHC staining in the cancerous tissue area compared with that in the normal tissue area. Quantitative data are presented as the mean ± SEM. ****P<0.0001. ARID1A, AT-rich interactive domain-containing protein 1A; H-score, histochemical scoring; NA, normal area; CA, cancerous area.

cells with *ARID1A* overexpression exhibited a more pronounced epithelial cell shape and appeared to exhibit slightly enhanced cell adhesion, resulting in a more rounded cellular structure when compared with the control cells (Fig. 2B). These results suggested that the changes in the physical structure of cells overexpressing *ARID1A*, which resembled an epithelial phenotype, may indicate that ARID1A has a role in inhibiting the spread of metastatic CRC by regulating biological mechanisms that contribute to EMT.

Overexpression of ARID1A induces alterations in cell junction molecules and the cytoskeleton in SW48 cells. Following the induction of *ARID1A* overexpression, there were notable alterations in the morphology of SW48 cells. Since the EMT process has been associated with a profound reorganization of the cytoskeleton, in order to weaken cell-cell attachment and strengthen cell-matrix adhesions (27), the present study observed the levels of ZO-1, E-cadherin and vimentin in SW48 cells overexpressing *ARID1A*. Immunofluorescence staining was used to determine the expression of ZO-1, E-cadherin and vimentin, and to evaluate their location in SW48 cells; quantitative analysis of immunofluorescence intensity is displayed in box-and-whisker plots. The results showed that ZO-1 and E-cadherin were present in the cell membrane, and were distinctly increased in *ARID1A*-overexpressing cells (Fig. 3A and B). By contrast, vimentin was detected in the cytoplasm and exhibited a decrease in cells with *ARID1A* overexpression (Fig. 3C). The expression levels of these proteins indicated that overexpression of *ARID1A* may affect cell shape remodeling, potentially resulting in suppressed EMT characteristics.

ARID1A overexpression influences the mRNA expression levels of EMT-related genes in SW48 cells. Subsequently, the present study explored the potential association between

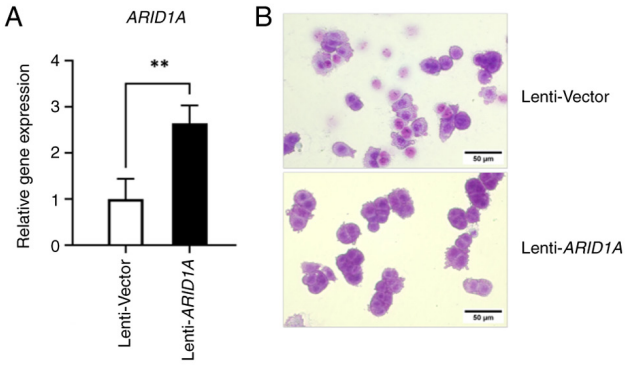

Figure 2. *ARID1A* overexpression induces epithelial phenotypes in SW48 cells. (A) RT-qPCR was performed to detect the mRNA expression levels of *ARID1A* in SW48 cells infected with the control lentivirus or a lentivirus expressing wildtype *ARID1A*. Data are presented as the mean ± SD. **P<0.01. (B) Overexpression of *ARID1A* led to alterations in the morphology of SW48 cells. Cells were stained with 0.4% crystal violet. Scale bar, 50 μm. *ARID1A*, AT-rich interactive domain-containing protein 1A.

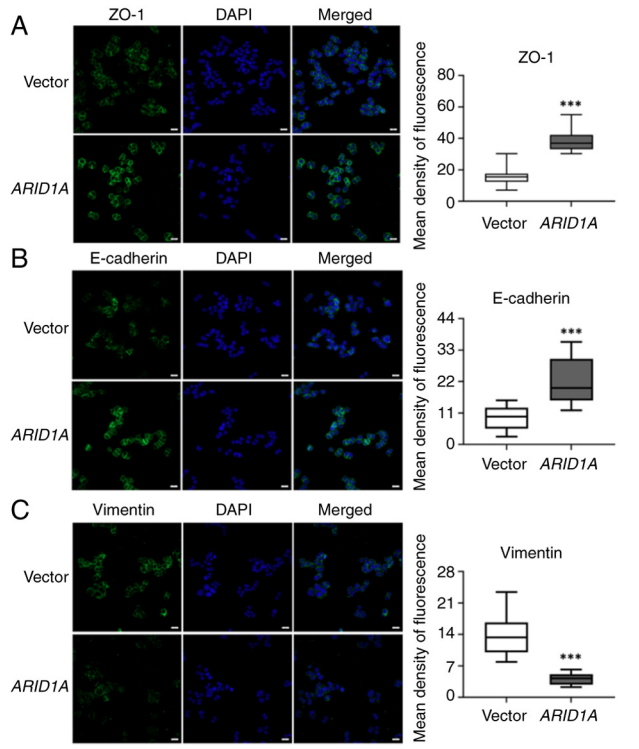

Figure 3. *ARID1A* overexpression enhances the expression of cell junction molecules and diminishes cytoskeletal arrangement. Immunofluorescence staining of cells showing the localization of (A) E-cadherin, (B) ZO-1 and (C) vimentin, using specific antibodies. Scale bar, 20 μm. Fluorescence intensity values are shown as the mean ± SEM. Box-and-whisker plots are presented; data points for each subject are the mean of three independent measurements. ***P<0.001 vs. vector control cells. *ARID1A*, AT-rich interacting domain-containing protein 1A; ZO-1, zonula occludens 1.

these changes and modulation of the EMT pathway in CRC cells mediated by ARID1A. First, the expression levels of the epithelial cell markers, *TJP1*/ZO-1 and *CDH1*/E-cadherin, and the mesenchymal markers, *VIM*/vimentin and *ZEB1*, were detected in the cells with *ARID1A* overexpression. RT-qPCR was carried out to detect the expression levels of these EMT-related genes in *ARID1A*-overexpressing SW48

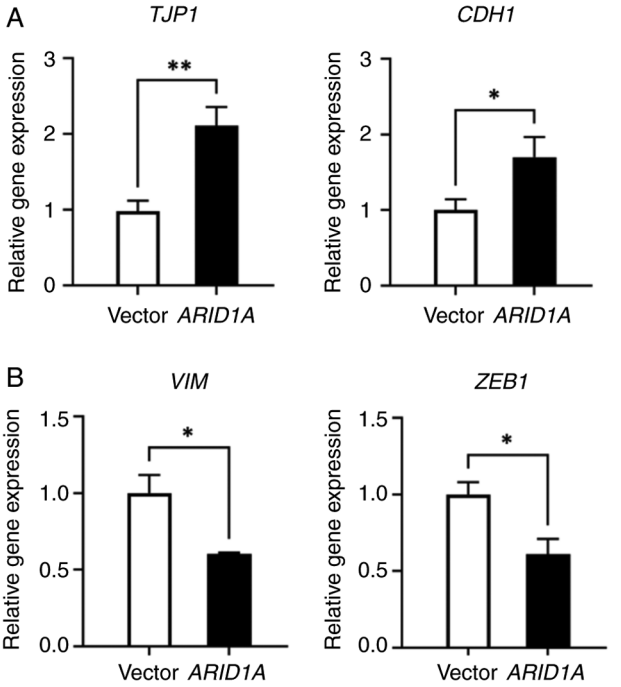

Figure 4. *ARID1A* overexpression influences the expression levels of EMT-related genes. (A) mRNA expression levels of epithelial markers, *TJP1*/ZO-1 and *CDH1*/E-cadherin. (B) mRNA expression levels of mesenchymal markers, *VIM*/vimentin and *ZEB1*. Reverse transcription-quantitative PCR was performed to detect the expression levels of EMT-related genes in SW48 cells overexpressing *ARID1A*. Data points for each subject are the mean of three independent measurements. Data are presented as the mean ± SEM. *P<0.05, **P<0.01. *ARID1A*, AT-rich interacting domain-containing protein 1A; EMT, epithelial-mesenchymal transition; *TJP1*/ZO-1, zonula occludens 1; *ZEB1*, zinc finger E-box binding homeobox 1.

cells (Fig. 4). The mRNA expression levels of the epithelial marker genes, *TJP1*/ZO-1 and *CDH1*/E-cadherin, were obviously upregulated (Fig. 4A). By contrast, there was a notable decrease in the expression levels of *VIM*/vimentin and *ZEB1*, both of which are considered mesenchymal marker genes (Fig. 4B). These RT-qPCR results demonstrated that ARID1A may negatively regulate the EMT process by influencing the expression of EMT-related genes in CRC.

ARID1A inhibits the motility and migration of SW48 cells. The progression of cancer is driven by cancer cell migration, which is a functional hallmark of EMT. To observe the effects of *ARID1A* overexpression on EMT-associated phenotypes, wound healing and cell migration assays were performed. The bright-field images from the wound healing experiment indicated that the motility of *ARID1A*-overexpressing cells was much slower when compared with control cells at each time point (Fig. 5A). The cell-free area in control cells remained at 58.83±6.68% at T48 and 39.74±9.78% at T72 (Fig. 5B). In cells overexpressing *ARID1A*, the cell-free area was 84.44±3.77 and 81.38±6.71% at T48 and T72, respectively (Fig. 5B). In addition, the cell wound closure rate was calculated as a reduction of cell-free area. As shown in Fig. 5C, the wound closure rate from T0 to T72 in the vector control group was obviously increased, whereas SW48 cells overexpressing *ARID1A* did not show a different wound closure rate over time (Fig. 5C). The results of the wound healing assay indicated that the motility

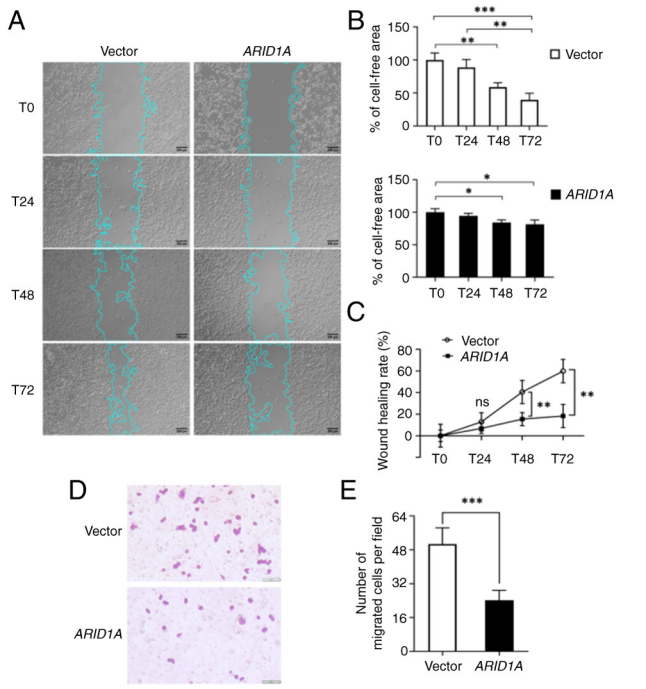

Figure 5. *ARID1A* overexpression suppresses the mobility and migration of human CRC cells. (A) Representative bright-field images of the wound healing assay showed the inhibitory effects of *ARID1A* overexpression on SW48 cell mobility. Original magnification, x100; scale bar, 200 μm. (B) Percentage of cell-free area at the indicated time points compared with the area at the start of the experiment (T0) was determined in vector control and *ARID1A*-overexpressing cells. (C) Wound closure rate was evaluated by measuring the remaining cell-free area and was expressed as a percentage of the initial cell-free area. (D) Measurement of the migratory activities of SW48 cells following *ARID1A* overexpression by Transwell cell migration assay. Cells were stained with 0.4% crystal violet. Original magnification, x400; scale bar, 50 μm. (E) ImageJ software was used to quantify the relative number of migratory cells. The results of three independent experiments are expressed as the mean ± SD. *P<0.05, **P<0.01, ***P<0.001. *ARID1A*, AT-rich interacting domain-containing protein 1A; ns, not significant.

of SW48 cells was markedly inhibited by *ARID1A* overexpression. Additionally, the Transwell cell migration assay revealed that *ARID1A* overexpression attenuated the migratory abilities of SW48 cells (Fig. 5D) and caused a significant reduction in the number of migrated cells (Fig. 5E). The wound healing and cell migration assays demonstrated that the strength of cell adhesion in SW48 cells overexpressing *ARID1A* may be due to ARID1A obstructing cell motility and migration related to EMT, which is a hallmark of malignancy.

Discussion

Recent studies have reported on the discovery of novel biomarkers and molecular targets in various types of cancer, with a particular emphasis on innovative diagnostic methods (28), the underlying molecular processes of cancer (29-33) and genetic changes (5,6,13). Dysregulation in gene expression serves a crucial role in cell proliferation and is a significant contributor to tumor development. Consequently, focusing on particular genes that are associated with CRC could offer a promising therapeutic strategy for its treatment (15). The *ARID1A* gene has been categorized as a novel tumor suppressor due to the association observed between *ARID1A*/BAF250a expression and various cancer types, including CRC (11-15). *ARID1A* has been identified as a highly mutated gene in CRC, with loss of its expression becoming increasingly significant as the TNM stage progresses, suggesting a strong association between ARID1A loss in CRC and the advancement of tumor progression and metastasis (16). Metastasis is a leading factor in the mortality of patients with CRC, and EMT is recognized as a pivotal process in cancer metastasis. The silencing of *ARID1A* has been reported to enhance migratory capabilities by promoting EMT in breast and gastric cancer cells (22,23). Although a previous study has reported that ARID1A knockdown results in upregulation of *VIM* and downregulation of *CDH1* in CRC cells (34), the EMT mechanisms that underlie the involvement of ARID1A in CRC metastasis have not been well characterized. The present study confirmed the low expression of ARID1A in CRC tissues, which was not assessed in previous research. Additionally, this study demonstrated the function of ARID1A in the processes of EMT and its association with ZEB1, a key transcriptional regulator of EMT in CRC. The findings showed that *ARID1A* overexpression can obstruct the EMT-like phenotype by increasing the expression of epithelial markers and decreasing those of mesenchymal markers, thereby inhibiting the EMT process of CRC cells and preventing CRC cell migration.

The initial findings of the current study indicated that the expression of ARID1A in human CRC tissue samples was lower compared with that in adjacent normal tissues. This confirms that ARID1A expression is commonly lost in human CRC, as reported in previous studies (16,35,36). In addition, the reduction of ARID1A has been associated with clinicopathological significance in patients with CRC. The loss of ARID1A has been reported to be significantly correlated with age, sex, location and tumor size (36), as well as distant metastasis and advanced TNM stage (16). Numerous studies have attempted to explore the fundamental molecular process behind the reduction of ARID1A expression in CRC. For example, loss of ARID1A expression has been shown to be associated with mismatch repair deficiency and somatic hypermethylation, as a key driver event in CRC (36). In addition, the deletion of *Arid1a* in mice has led to the formation of invasive adenocarcinoma in the colon (37). However, the molecular mechanisms underlying the role of ARID1A in CRC metastasis remain to be elucidated. EMT is a crucial element in the process of tumor metastasis and invasion, playing a pivotal role in the progression of cancer, notably in CRC (21). Hence, the present study focused on assessing the role of ARID1A in the EMT pathway, which presents an intriguing area of research in the context of cell migration, a metastatic feature of cancer.

A recent study revealed diverse mRNA expression levels of *ARID1A* in different CRC cell lines, ranging from high levels in HCT116 and HT-29/219 cells to nearly undetectable levels in SW48 cells (35). Therefore, this facilitated the design of the *ARID1A* overexpression experimental model in SW48 cells. Transduction of a lentivirus containing the human full-length *ARID1A* sequence had a significant impact on cellular morphological alterations, leading to a greater prevalence of cells with an epithelial phenotype and enhanced cell-to-cell contact. Since epithelial cells exhibit polarity from their apical to basal surfaces, establishing adhesion and communication among themselves via specialized intercellular junctions (38), the present study revealed that the tight junction molecule, ZO-1, and the adherens junction

molecule, E-cadherin (epithelial cadherin), were significantly increased in cells overexpressing *ARID1A*. By contrast, the intermediate filament protein, vimentin, was decreased. Key events in EMT include the dissolution of epithelial cell-cell junctions, loss of apical-basal polarity, reorganization of the cytoskeletal architecture and alterations in cellular morphology (27,30,39). Therefore, the present results indicated that the overexpression of *ARID1A* could potentially inhibit EMT-like characteristics. These results were confirmed by the detection of the mRNA expression levels of EMT-related genes. *ARID1A*-overexpressing cells exhibited upregulation of the epithelial markers *TJP1*/ZO-1 and *CDH1*/E-cadherin, whereas the mesenchymal markers *VIM*/vimentin and *ZEB1* were downregulated. The EMT process is distinguished by the loss of epithelial markers, such as E-cadherin, and the gain of mesenchymal markers, such as vimentin (40,41). Several studies have reported that as most types of cancer progresses, there is an observed increase in vimentin levels (31,41), while E-cadherin levels tend to decrease (41,42). Regarding the present data, *ARID1A* overexpression enhanced E-cadherin levels and reduced vimentin levels, indicating the functional role of ARID1A in negatively regulating the EMT process. Consequently, the migratory capabilities of cells overexpressing *ARID1A* were suppressed.

The present findings are consistent with the findings of previous reports. In a previous study, *ARID1A* silencing was shown to induce E-cadherin downregulation, enhancing gastric cancer cell migration and invasion (23). Baldi *et al* (34) reported that *ARID1A* deficiency could promote cell proliferation and migration via *VIM* activation and *CDH1* suppression in colon cancer. In addition to E-cadherin and vimentin, other EMT-related markers, *TJP1*/ZO-1 and *ZEB1* were also revealed to be associated with ARID1A-regulated EMT. ZO-1 is essential for tight junction formation. The tight junctions of cells disintegrate during EMT, accompanied by reduced levels of ZO-1 expression (38). Zhang *et al* (43) detected a decline in ZO-1 expression in hepatocellular carcinoma. Accordingly, overexpression of ZO-1 suppressed HepG2 cell proliferation. ZEB1 has been recognized as a key transcriptional regulator of EMT, and inhibiting ZEB1 has been reported to reduce the migration and invasion of prostate cancer (29). Despite these findings, to the best of our knowledge, the present study is the first to report that *ARID1A* overexpression may inhibit CRC cell migration through the suppression of the EMT process by enhancing ZO-1 expression while decreasing ZEB1 expression levels. Recently, our proteomic analysis investigation demonstrated that the overexpression of *ARIDA* had a notable impact on the modification of multiple proteins associated with the Wnt signaling pathway in CRC cells (44). The activation of Wnt signaling in colon cancer is responsible for driving tumorigenesis and facilitating advanced metastasis through the promotion of the EMT program (32). However, the present study did not investigate the involvement of the Wnt signaling pathway in the regulation of EMT in CRC. Future research involving gene knockdown experiments, the use of specific inhibitors against the Wnt signaling pathway, and immunohistochemistry for Wnt-related proteins is required to enhance the understanding of the mechanisms observed in the present study.

In conclusion, the findings of the present study indicated that expression of the tumor suppressor ARID1A is frequently lost in CRC tissues. The *in vitro* experiments demonstrated that ARID1A may have the potential to counteract EMT-like characteristics and cell migration by modifying the expression of EMT-related genes. In simpler terms, ARID1A might impede the EMT process in CRC, leading to the inhibition of malignant progression. Consequently, additional investigations are necessary to identify which EMT pathways are regulated by ARID1A, and to establish a stronger connection between the clinical treatment of CRC and the utilization of ARID1A as a biomarker and therapeutic target for CRC metastasis.

Acknowledgements

The authors would like to thank Mr. Olalekan Isreal Aiikulola (Faculty of Medical Science, Naresuan University, Phitsanulok, Thailand) for providing an English editing service. Additionally, the authors would like to thank Dr Ratirat Samol (Unit of Pathology, Sawanpracharak Hospital, Nakhon Sawan, Thailand), for providing the FFPE tissue blocks.

Funding

This research received funding support from the National Science, Research, and Innovation Fund via the Program Management Unit for Human Resources & Institutional Development, Research and Innovation (grant no. B05F640168).

Availability of data and materials

The data generated in the present study may be requested from the corresponding author.

Authors' contributions

SW contributed to the conception and design of the study, conducted experiments, performed data analysis and visualization, and was a major contributor to manuscript writing. SA, KS and WM participated in experiments and data analysis. NS contributed to the conception and design of the study, data analysis, supervision, funding acquisition and manuscript editing. SW and NS confirm the authenticity of all the raw data. All authors read and approved the final version of the manuscript.

Ethics approval and consent to participate

All procedures performed involving human participants adhered to the ethical guidelines set by the institutional and/or national research committee, as well as The 1964 Declaration of Helsinki and its subsequent amendments, or equivalent ethical standards. The study received authorization from the Human Ethics Review Board of Sawanpracharak Hospital (approval no. 16/2560) and the Naresuan University Ethical Committee for Human Research (approval no. P1-0191/2564; certificate of approval no. 178/2021). Written informed consent was obtained from all subjects involved in the study.

Patient consent for publication

Not applicable.

Competing interest

The authors declare that they have no competing interests.

References

1. Siegel RL, Miller KD, Wagle NS and Jemal A: Cancer statistics, 2023. CA Cancer J Clin 73: 17-48, 2023.
2. Siegel RL, Wagle NS, Cercek A, Smith RA and Jemal A: Colorectal cancer statistics, 2023. CA Cancer J Clin 73: 233-254, 2023.
3. Brenner H, Heisser T, Cardoso R and Hoffmeister M: Reduction in colorectal cancer incidence by screening endoscopy. Nat Rev Gastroenterol Hepatol 21: 125-133, 2024.
4. Bhupender S and Chhikara KP: Global Cancer Statistics 2022: The trends projection analysis. Chem Biol Lett 10: 451, 2023.
5. Biller LH and Schrag D: Diagnosis and treatment of metastatic colorectal cancer: A review. JAMA 325: 669-685, 2021.
6. Malki A, ElRuz RA, Gupta I, Allouch A, Vranic S and Al Moustafa AE: Molecular mechanisms of colon cancer progression and metastasis: Recent insights and advancements. Int J Mol Sci 22: 130, 2020.
7. Vogelstein B, Fearon ER, Hamilton SR, Kern SE, Preisinger AC, Leppert M, Smits AM and Bos JL: Genetic alterations during colorectal-tumor development. N Engl J Med 319: 525-532, 1988.
8. Wilson BG and Roberts CWM: SWI/SNF nucleosome remodellers and cancer. Nat Rev Cancer 11: 481-492, 2011.
9. Reisman D, Glaros S and Thompson E: The SWI/SNF complex and cancer. Oncogene 28: 1653-1668, 2009.
10. Shain AH and Pollack JR: The spectrum of SWI/SNF mutations, ubiquitous in human cancers. PLoS One 8: e55119, 2013.
11. Wiegand KC, Shah SP, Al-Agha OM, Zhao Y, Tse K, Zeng T, Senz J, McConechy MK, Anglesio MS, Kalloger SE, *et al*: ARID1A mutations in endometriosis-associated ovarian carcinomas. N Engl J Med 363: 1532-1543, 2010.
12. Mamo A, Cavallone L, Tuzmen S, Chabot C, Ferrario C, Hassan S, Edgren H, Kallioniemi O, Aleynikova O, Przybytkowski E, *et al*: An integrated genomic approach identifies ARID1A as a candidate tumor-suppressor gene in breast cancer. Oncogene 31: 2090-2100, 2012.
13. Guichard C, Amaddeo G, Imbeaud S, Ladeiro Y, Pelletier L, Maad IB, Calderaro J, Bioulac-Sage P, Letexier M, Degos F, *et al*: Integrated analysis of somatic mutations and focal copy-number changes identifies key genes and pathways in hepatocellular carcinoma. Nat Genet 44: 694-698, 2012.
14. Streppel MM, Lata S, DelaBastide M, Montgomery EA, Wang JS, Canto MI, Macgregor-Das AM, Pai S, Morsink FH, Offerhaus GJ, *et al*: Next-generation sequencing of endoscopic biopsies identifies ARID1A as a tumor-suppressor gene in Barrett's esophagus. Oncogene 33: 347-357, 2014.
15. Muzny DM, Bainbridge MN, Chang K, Dinh HH, Drummond JA, Fowler G, Kovar CL, Lewis LR, Morgan MB, Newsham IF, *et al*: Comprehensive molecular characterization of human colon and rectal cancer. Nature 487: 330-337, 2012.
16. Wei XL, Wang DS, Xi SY, Wu WJ, Chen DL, Zeng ZL, Wang RY, Huang YX, Jin Y, Wang F, *et al*: Clinicopathologic and prognostic relevance of ARID1A protein loss in colorectal cancer. World J Gastroenterol 20: 18404-18412, 2014.
17. Ye J, Zhou Y, Weiser MR, Gönen M, Zhang L, Samdani T, Bacares R, DeLair D, Ivelja S, Vakiani E, *et al*: Immunohistochemical detection of ARID1A in colorectal carcinoma: Loss of staining is associated with sporadic microsatellite unstable tumors with medullary histology and high TNM stage. Hum Pathol 45: 2430-2436, 2014.
18. Toiyama Y, Yasuda H, Saigusa S, Tanaka K, Inoue Y, Goel A and Kusunoki M: Increased expression of Slug and Vimentin as novel predictive biomarkers for lymph node metastasis and poor prognosis in colorectal cancer. Carcinogenesis 34: 2548-2557, 2013.
19. Ye X and Weinberg RA: Epithelial-Mesenchymal plasticity: A central regulator of cancer progression. Trends Cell Biol 25: 675-686, 2015.
20. Brabletz T, Kalluri R, Nieto MA and Weinberg RA: EMT in cancer. Nat Rev Cancer 18: 128-134, 2018.
21. Gurzu S, Silveanu C, Fetyko A, Butiurca V, Kovacs Z and Jung I: Systematic review of the old and new concepts in the epithelial-mesenchymal transition of colorectal cancer. World J Gastroenterol 22: 6764-6775, 2016.
22. Wang T, Gao X, Zhou K, Jiang T, Gao S, Liu P, Zuo X and Shi X: Role of ARID1A in epithelial-mesenchymal transition in breast cancer and its effect on cell sensitivity to 5-FU. Int J Mol Med 46: 1683-1694, 2020.
23. Yan HB, Wang XF, Zhang Q, Tang ZQ, Jiang YH, Fan HZ, Sun YH, Yang PY and Liu F: Reduced expression of the chromatin remodeling gene ARID1A enhances gastric cancer cell migration and invasion via downregulation of E-cadherin transcription. Carcinogenesis 35: 867-876, 2014.
24. Livak KJ and Schmittgen TD: Analysis of relative gene expression data using real-time quantitative PCR and the 2(-Delta Delta C(T)) method. Methods 25: 402-408, 2001.
25. Tian X, Wei Z, Wang J, Liu P, Qin Y and Zhong M: MicroRNA-429 inhibits the migration and invasion of colon cancer cells by targeting PAK6/cofilin signaling. Oncol Rep 34: 707-714, 2015.
26. Schneider CA, Rasband WS and Eliceiri KW: NIH Image to ImageJ: 25 years of image analysis. Nat Methods 9: 671-675, 2012.
27. Yilmaz M and Christofori G: EMT, the cytoskeleton, and cancer cell invasion. Cancer Metastasis Rev 28: 15-33, 2009.
28. Wang R, Yang S, Wang M, Zhou Y, Li X, Chen W, Liu W, Huang Y, Wu J and Cao J: A sustainable approach to universal metabolic cancer diagnosis. Nat Sustainability 7: 602-615, 2024.
29. Graham TR, Zhau HE, Odero-Marah VA, Osunkoya AO, Kimbro KS, Tighiouart M, Liu T, Simons JW and O'Regan RM: Insulin-like growth factor-I-dependent up-regulation of ZEB1 drives epithelial-to-mesenchymal transition in human prostate cancer cells. Cancer Res 68: 2479-2488, 2008.
30. Leggett SE, Hruska AM, Guo M and Wong IY: The epithelial-mesenchymal transition and the cytoskeleton in bioengineered systems. Cell Commun Signal 19: 32, 2021.
31. Niknami Z, Eslamifar A, Emamirazavi A, Ebrahimi A and Shirkoohi R: The association of vimentin and fibronectin gene expression with epithelial-mesenchymal transition and tumor malignancy in colorectal carcinoma. EXCLI J 16: 1009-1017, 2017.
32. Zhao H, Ming T, Tang S, Ren S, Yang H, Liu M, Tao Q and Xu H: Wnt signaling in colorectal cancer: Pathogenic role and therapeutic target. Mol Cancer 21: 144, 2022.
33. Yang Q, Huang W, Hsu JC, Song L, Sun X, Li C, Cai W and Kang L: CD146-targeted nuclear medicine imaging in cancer: State of the art. View (Beijing) 4: 20220085, 2023.
34. Baldi S, Zhang Q, Zhang Z, Safi M, Khamgan H, Wu H, Zhang M, Qian Y, Gao Y, Shopit A, *et al*: ARID1A downregulation promotes cell proliferation and migration of colon cancer via VIM activation and CDH1 suppression. Cell Mol Med 26: 5984-5997, 2022.
35. Erfani M, Hosseini SV, Mokhtari M, Zamani M, Tahmasebi K, Alizadeh Naini M, Taghavi A, Carethers JM, Koi M, Brim H, *et al*: Altered ARID1A expression in colorectal cancer. BMC Cancer 20: 350, 2020.
36. Chou A, Toon CW, Clarkson A, Sioson L, Houang M, Watson N, DeSilva K and Gill AJ: Loss of ARID1A expression in colorectal carcinoma is strongly associated with mismatch repair deficiency. Hum Pathol 45: 1697-1703, 2014.
37. Mathur R, Alver BH, San Roman AK, Wilson BG, Wang X, Agoston AT, Park PJ, Shivdasani RA and Roberts CW: ARID1A loss impairs enhancer-mediated gene regulation and drives colon cancer in mice. Nat Genet 49: 296-302, 2017.
38. Huang RYJ, Guilford P and Thiery JP: Early events in cell adhesion and polarity during epithelial-mesenchymal transition. J Cell Sci 125: 4417-4422, 2012.
39. Lamouille S, Xu J and Derynck R: Molecular mechanisms of epithelial-mesenchymal transition. Nat Rev Mol Cell Biol 15: 178-196, 2014.
40. Gout S and Huot J: Role of cancer microenvironment in metastasis: Focus on colon cancer. Cancer Microenviron 1: 69-83, 2008.
41. Xiao S, Liu L, Lu X, Long J, Zhou X and Fang M: The prognostic significance of bromodomain PHD-finger transcription factor in colorectal carcinoma and association with vimentin and E-cadherin. J Cancer Res Clin Oncol 141: 1465-1474, 2015.
42. Kolijn K, Verhoef EI and van Leenders GJ: Morphological and immunohistochemical identification of epithelial-to-mesenchymal transition in clinical prostate cancer. Oncotarget 6: 24488-24498, 2015.
43. Zhang X, Wang L, Zhang H, Tu F, Qiang Y and Nie C: Decreased expression of ZO-1 is associated with tumor metastases in liver cancer. Oncol Lett 17: 1859-1864, 2019.
44. Aluksanasuwan S, Somsuan K, Wanna-Udom S, Roytrakul S, Morchang A, Rongjumnong A and Sakulsak N: Proteomic insights into the regulatory function of ARID1A in colon cancer cells. Oncology Letters 28: 392, 2024.